


ARTICLE



A diet-induced murine model for non-alcoholic fatty liver disease with obesity and insulin resistance that rapidly develops steatohepatitis and fibrosis

Takafumi Sakuma¹, Masato Nakamura¹ [✉], Tetsuhiro Chiba¹, Terunao Iwanaga¹, Motoyasu Kan¹, Ryuta Kojima¹, Junjie Ao¹, Yaojia Ma¹, Hidemi Unozawa¹, Naoto Fujita¹, Kengo Kanayama¹, Hiroaki Kanzaki¹, Keisuke Koroki¹, Kazufumi Kobayashi^{1,2}, Ryo Nakagawa¹, Naoya Kanogawa¹, Soichiro Kiyono¹, Takayuki Kondo¹, Tomoko Saito¹, Sadahisa Ogasawara^{1,2}, Shingo Nakamoto¹, Ryoosuke Muroyama³, Jun Kato¹, Takashi Kishimoto⁴ and Naoya Kato¹

© The Author(s), under exclusive licence to United States and Canadian Academy of Pathology 2022

Non-alcoholic fatty liver disease (NAFLD) has become the leading cause of chronic liver disease worldwide. Patients with NAFLD often suffer steatohepatitis, which can progress to cirrhosis and hepatocellular carcinoma. The presence of visceral obesity or type 2 diabetes mellitus (T2DM) is a major risk factor and potential therapeutic target for NAFLD. The establishment of animal models with these metabolic comorbidities and with the rapid progression of the disease is needed for developing treatments for NAFLD but remains to be achieved. In the present study, KK-A^y mice, widely used as T2DM models, or C57BL6 mice were fed a high-fat, high-fructose, and high-cholesterol diet supplemented with cholic acid (NAFLD diet). The KK-A^y mice fed a NAFLD diet exhibited remarkable obesity and insulin resistance. A prominent accumulation of triglycerides and cholesterol in the liver was observed at 4 weeks. These mice developed steatohepatitis at 4 weeks and fibrosis at 12 weeks. In contrast, C57BL6 mice fed a NAFLD diet remained lean, although they still developed steatohepatitis and fibrosis. In summary, we established a diet-induced murine NAFLD model with the rapid development of steatohepatitis and fibrosis, bearing obesity and insulin resistance. This model could be useful as preclinical models for drug development of NAFLD.

Laboratory Investigation (2022) 102:1150–1157; <https://doi.org/10.1038/s41374-022-00807-6>

INTRODUCTION

Non-alcoholic fatty liver disease (NAFLD) is becoming the leading cause of chronic liver disease worldwide. A considerable proportion of patients with NAFLD suffers from steatohepatitis [namely, non-alcoholic steatohepatitis (NASH)], which could progress to cirrhosis, and later to hepatocellular carcinoma (HCC).

The prevalence of NAFLD increases not only in the Western world but also in Asian countries^{1,2}. The global prevalence of NAFLD and NASH in the general population has been estimated to reach 25% and 3–5%, respectively^{3,4}. In the USA, NAFLD has become the second leading indication for liver transplantation⁵ and the second leading cause of HCC among patients listed for liver transplantation⁶. Furthermore, a recent model analysis reported that the prevalence of NASH will increase by 15–56% and the incidence of advanced liver disease and liver-related mortality will more than double by 2030⁷.

Although the conquest of NAFLD is urgently needed, the establishment of treatment methods for NAFLD is still a daunting task. The improvement of animal models is one of the requirements for the establishment of a treatment. Various factors, such as metabolic profile, lifestyles, gender, age, ethnicity, and genetic background, affect the incidence and disease progression

of NAFLD. The complexity of disease makes dietary models preferable as preclinical models to genetic models that rely on one specific gene knockout. Among risk factors, the presence of visceral obesity or type 2 diabetes mellitus (T2DM) are particularly important because they can predispose to liver fibrosis, HCC, and death^{8–10}. The stage of fibrosis is also essential due to its strong association with mortality in patients with NAFLD¹¹. Therefore, preclinical models of NAFLD should represent obesity, T2DM or insulin resistance, and liver fibrosis. While some dietary murine model could represent these phenotypes, they develop only mild steatohepatitis and fibrosis after taking long-term interventions. The combination of dietary interventions with chemical treatment, such as carbon tetrachloride (CCl₄), could enhanced progression of steatohepatitis and fibrosis, although it would impair weight gain and insulin resistance¹².

KK-A^y mice are widely used as T2DM models. These mice possess the genetic background of KK mice, a polygenetic diabetic murine strain. The ectopic expression of agouti protein in KK-A^y mice induces hyperleptinemia and leptin resistance¹³ by antagonizing of the melanocortin receptor-4¹⁴ and causing hyperphagia, resulting in marked obesity, hyperlipidemia, and insulin resistance¹⁵.

¹Department of Gastroenterology, Chiba University, Graduate School of Medicine, Chiba 260-8677, Japan. ²Translational Research and Development Center, Chiba University Hospital, Chiba 260-8677, Japan. ³Department of Molecular Virology, Chiba University, Graduate School of Medicine, Chiba 260-8677, Japan. ⁴Department of Molecular Pathology, Chiba University, Graduate School of Medicine, Chiba 260-8677, Japan. ✉email: nakamura-ma@chiba-u.jp

Received: 20 December 2021 Revised: 8 May 2022 Accepted: 9 May 2022

Published online: 28 May 2022

In this study, we report a murine model for NAFLD using KK-A^y mice fed a high-fat, high-fructose, and high-cholesterol diet supplemented with cholic acid. Our model developed severe obesity, insulin resistance and dyslipidemia. They also exhibited marked steatohepatitis within 4 weeks and significant fibrosis within 12 weeks.

MATERIALS AND METHODS

Animals

All animals received humane care according to the criteria outlined in the "Guide for the Care and Use of Laboratory Animals." Male KK-A^y/TaJcl mice and male C57BL/6Jcl mice were purchased from CLEA Japan (Tokyo, Japan). All mice were housed in a 12 h light/dark cycle. They were euthanized at varying time points after the initiation of dietary intervention.

Dietary intervention

Mice (6 weeks old) were randomly fed ad libitum a NAFLD diet containing 40 kcal% fat, 20 kcal% fructose, 2% cholesterol, and 0.5% cholic acid (Research Diets, New Brunswick, NJ, USA; #D19061001) or a standard chow diet (Research Diets; #D09100304N).

Serum analysis

Serum alanine aminotransferase (ALT), total cholesterol, LDL cholesterol (LDL-C), HDL cholesterol (HDL-C), and triglyceride levels were measured by Oriental Yeast (Tokyo, Japan). Fasting blood glucose levels were measured with a blood glucose meter (FreeStyle Freedom Light; NIPRO, Osaka, Japan). Fasting serum insulin levels were measured using the Ultra Sensitive Mouse Insulin ELISA Kit, according to the manufacturer's instructions (Morinaga Institute of Biological Science, Kanagawa, Japan). The homeostatic model assessment for insulin resistance (HOMA-IR) was calculated as previously described¹⁶.

Quantification of the hepatic lipid content

Total hepatic lipid was extracted from liver specimen snap frozen in liquid nitrogen using a protocol adapted from Folch et al.¹⁷. Total cholesterol and triglyceride were measured using enzyme assay. All procedures were performed by Skylight Biotech (Akita, Japan).

Liver histology

Formalin-fixed, paraffin-embedded liver sections were stained with hematoxylin and eosin (H&E) for assessment of liver histology and with Sirius Red for assessment of fibrosis. Frozen liver sections were stained with Oil Red O for assessment of steatosis. Preparation and staining of liver sections were performed by Biopathology Institute (Oita, Japan). Steatosis, lobular inflammation, hepatocyte ballooning and fibrosis were assessed by two expert hepatologists who were not blinded to the dietary condition in consultation with an expert pathologist. Histological scoring of steatosis and inflammation was performed according to the grading system for rodent NAFLD, reported by Liang et al.¹⁸. Specifically, the macrovesicular steatosis, microvesicular steatosis and hepatocellular hypertrophy were graded based on the percentage of involved hepatocytes, into the following categories; 0 (<5%), 1 (5–33%), 2 (34–66%) and 3 (>66%). Hepatocellular hypertrophy was defined as cellular enlargement more than 1.5 times the normal hepatocyte diameter. Inflammation was graded based on the number of inflammatory foci per field (100×), into the following categories; 0 (<0.5 foci), 1 (0.5–1.0 foci), 2 (1.0–2.0 foci) and 3 (>2.0 foci). Histological staging of fibrosis was evaluated according to the scoring system by Kleiner et al.¹⁹. Specifically, fibrosis was scored as stage 0 (no fibrosis), stage 1a (mild perisinusoidal fibrosis), stage 1b (moderate perisinusoidal fibrosis), stage 1c (portal/periportal fibrosis), stage 2 (perisinusoidal and portal/periportal fibrosis), stage 3 (bridging fibrosis), and stage 4 (cirrhosis). The tumor histology was evaluated by an expert pathologist.

Immunohistochemistry

Formalin-fixed, paraffin-embedded liver sections were incubated with primary antibodies against F4/80 (BMA Biomedicals, Augst, Switzerland; #T-2028) and actin alpha 2 (ACTA2) (Agilent, Santa Clara, CA, USA; #M0851). Preparation and staining of liver sections were performed by Kyodo Byori (Kobe, Japan).

Quantification of the fibrotic area

Scanning and image processing of whole Sirius Red-stained liver sections were performed as described above. The Sirius Red-positive area was extracted and calculated as percentage of the total area. Whole liver sections were scanned by a fluorescence microscope BZ-X800 with an advanced observation module BZ-H4XD (Keyence, Osaka, Japan) at ×40 magnification. Image processing was performed using the BZ-X analyzer BZ-H4A and hybrid cell count module BZ-H4C (Keyence). The staining-positive area was extracted and calculated as percentage of the total area.

Quantitative polymerase chain reaction

Liver specimens were treated with Allprotect Tissue Reagent (Qiagen, Venlo, Netherlands) and stored at −80 °C until analysis. Total RNA was isolated with QIA Shredder and miRNeasy Mini kits (Qiagen). Complementary DNA (cDNA) was synthesized using a PrimeScript RT Reagent kit (Takara BIO, Shiga, Japan). Gene expression levels were measured by quantitative PCR with TB Green Premix Ex Taq (Takara BIO) and a ABI7300 Real-Time PCR system (Applied Biosystems, Foster City, CA, USA). The relative expression was normalized by glyceraldehyde 3-phosphate dehydrogenase (Gapdh) expression as an endogenous control. Data analysis was performed using the 2^{−ddCt} (comparative cycle threshold) methods. The sequences of primers used in this study are shown in Table S1.

Statistics

Continuous data are expressed as medians with interquartile ranges unless otherwise stated. Statistical significance for comparison between the NAFLD group and the control group was evaluated using the Wilcoxon test unless otherwise stated. Statistical significance for comparison between all groups was evaluated using the Steel-Dwass test. Two-sided *p* values < 0.05 were considered statistically significant. Statistical analysis was performed using JMP Pro 15 software (SAS Institute, Cary, NC, USA). Graphs were made using GraphPad Prism 8 (GraphPad Software, La Jolla, CA, USA).

Study approval

All procedures were performed according to protocols approved by the Animal Care and Use Committee of the Chiba University.

RESULTS

KK-A^y mice fed a NAFLD diet develop severe obesity, dyslipidemia and insulin resistance

Representative pictures of the appearance of mice are shown in Fig. S1 and Fig. 1A. KK-A^y mice fed a NAFLD diet (KK-A^y/NAFLD) demonstrated marked obesity compared to KK-A^y mice fed a standard chow diet (KK-A^y/control) whereas C57BL/6 mice fed a NAFLD diet (B6/NAFLD) showed no difference from C57BL/6 mice fed a control chow diet (B6/control). The KK-A^y/NAFLD group developed significant weight gain from 1 week after the initiation of dietary intervention although food and caloric intake were significantly decreased. The B6/NAFLD group showed almost the same levels of weight gain, food intake and caloric intake (Fig. 1B and Fig. S2A, B). The weight of mesenteric fat was significantly increased in the KK-A^y/NAFLD group at 12 weeks, but not in the B6/NAFLD group compared to their respective controls (Fig. 1C).

Serum LDL-C was significantly increased in both the B6/NAFLD group and the KK-A^y/NAFLD group at 4 and 12 weeks (Fig. 1D). Total cholesterol was also significantly increased in both B6/NAFLD and KK-A^y/NAFLD groups at 12 weeks (Fig. S3A). Serum HDL-C was decreased in both groups at 4 weeks and the B6/NAFLD group at 12 weeks (Fig. S3B). Serum triglycerides were decreased in both B6/NAFLD and KK-A^y/NAFLD groups at 4 and 12 weeks (Fig. 1E).

Decreased HOMA-IR were observed at 12 weeks in the B6/NAFLD group (Fig. 1F). The basal blood glucose level was decreased without a significant change in the basal insulin level (Fig. S3C, D). It might be due to cholic acid supplemented in a NAFLD diet. The KK-A^y is a murine strain that shows obesity and insulin resistance with feeding on a standard chow diet. High

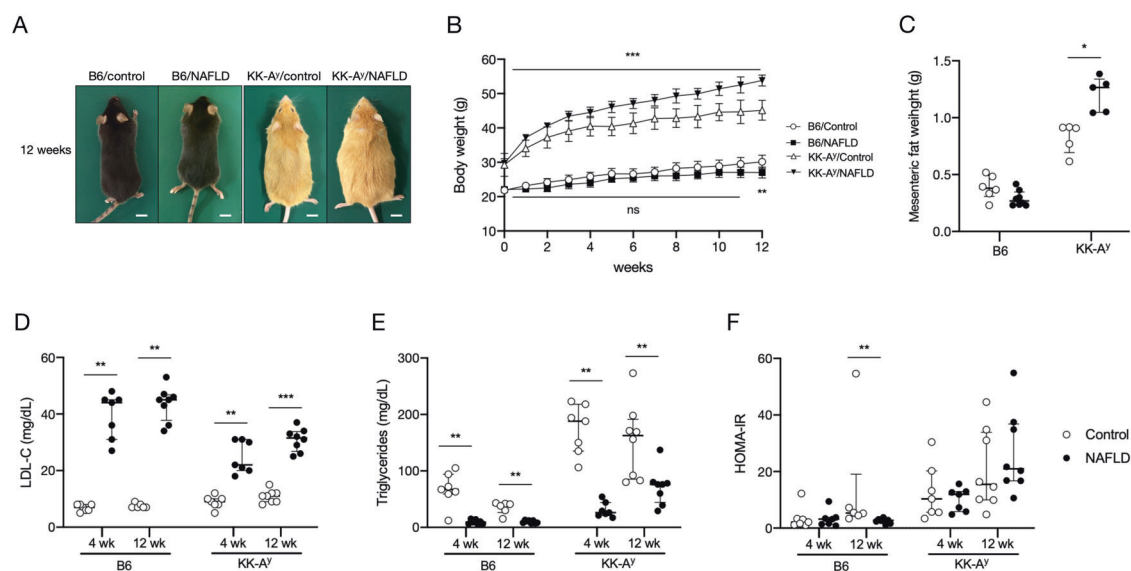


Fig. 1 Metabolic features of mice with dietary intervention. C57BL6/J mice or $KK-A^Y$ mice were fed a standard chow diet or a NAFLD diet for up to 12 weeks. **A** Representative appearance of mice at 12 weeks after dietary intervention. Scale bar, 10 mm. **B** Transition of body weight for 12 weeks. **C** Weight of mesenteric fat at 12 weeks. **D** Serum LDL cholesterol, **(E)** serum triglyceride, and **(F)** HOMA-IR at 4 and 12 weeks. Continuous data are expressed as median with interquartile range for the 6–8 mice per group. The NAFLD group and control groups were compared using the Wilcoxon test. $p < 0.05$, $^{*}p < 0.01$, $^{***}p < 0.001$. ns not significant.

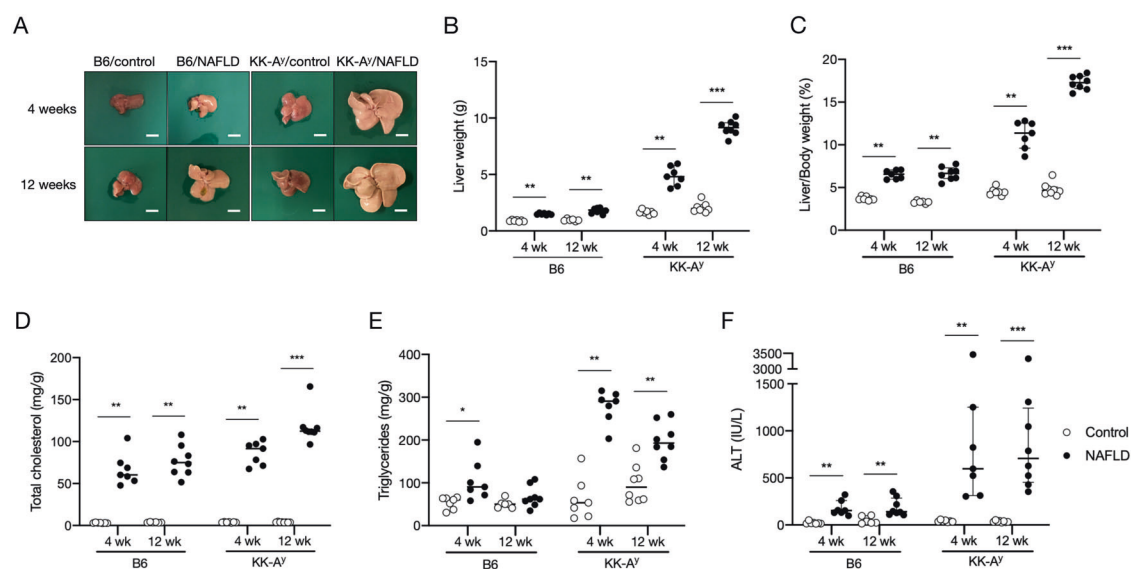


Fig. 2 Lipid profile in the liver of mice with dietary intervention. **A** The representative appearance of liver at 4 and 12 weeks after dietary intervention. Scale bar, 10 mm. **B** Liver weight, **(C)** liver per body weight ratio, and **(F)** serum ALT. Continuous data are expressed as median with interquartile range for 6–8 mice per group. **D** Total cholesterol content and **(E)** triglyceride content in the liver. Continuous data are expressed as mean for 6–8 mice per group. The NAFLD and control groups were compared by Wilcoxon test. $p < 0.05$, $^{*}p < 0.01$, $^{***}p < 0.001$.

HOMA-IR showed the presence of insulin resistance in the $KK-A^Y$ /control group (Fig. 1F). There were no differences in basal blood glucose, basal insulin, and HOMA-IR between the $KK-A^Y$ /NAFLD group and the $KK-A^Y$ /control group, indicating that cholic acid supplementation had no influence on insulin resistance in $KK-A^Y$ mice (Fig. 1F and Fig. S3C, D).

Dietary intervention rapidly causes fat accumulation and steatohepatitis in mice

Mice fed a NAFLD diet developed fatty liver and hepatomegaly at 4 and 12 weeks, especially in $KK-A^Y$ mice (Fig. 2A). Some mice in the $KK-A^Y$ /control group showed slight fatty changes of the liver.

Liver weight and liver to body weight increased at 4 and 12 weeks in both mouse strains, and the change was prominent in the $KK-A^Y$ /NAFLD group (Fig. 2B, C). Hepatic total cholesterol was increased at 4 and 12 weeks in both mouse strains, and hepatic triglycerides were increased at 4 and 12 weeks in $KK-A^Y$ mice and at 4 weeks in C57BL/6 mice compared to their respective controls (Fig. 2D, E). Dietary intervention also led to a significant increase of serum ALT at 4 and 12 weeks in both mouse strains (Fig. 2F).

Representative images of liver sections stained with hematoxylin-eosin and Oil Red O were shown (Fig. 3A–C). Hepatocyte ballooning was not observed in either the $KK-A^Y$ /NAFLD group or the B6/NAFLD group. The both mice strains fed a

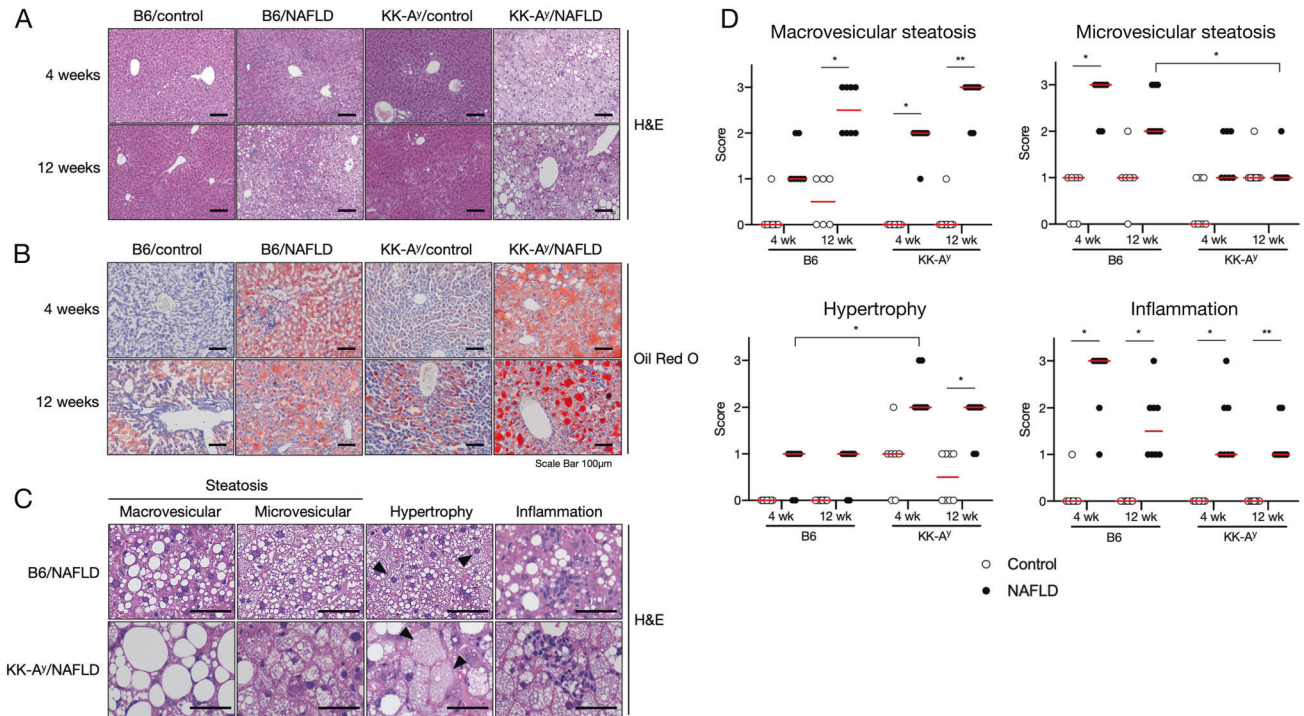


Fig. 3 Histological features of mice with dietary intervention. Representative images of liver sections stained with (A) hematoxylin-eosin (H&E) and (B) Oil Red O at 4 and 12 weeks. Scale bar, 100 μ m. C Representative images of macrovesicular steatosis, microvesicular steatosis, hypertrophy and inflammation in liver sections stained with H&E at 12 weeks. Scale bar, 50 μ m. D Histological scoring of steatosis and inflammation according to the grading system for rodent NAFLD. Each score was plotted with median (red bar) for 6–8 mice per group. All groups were compared using the Steel-Dwass test. * $p < 0.05$, ** $p < 0.01$, *** $p < 0.001$.

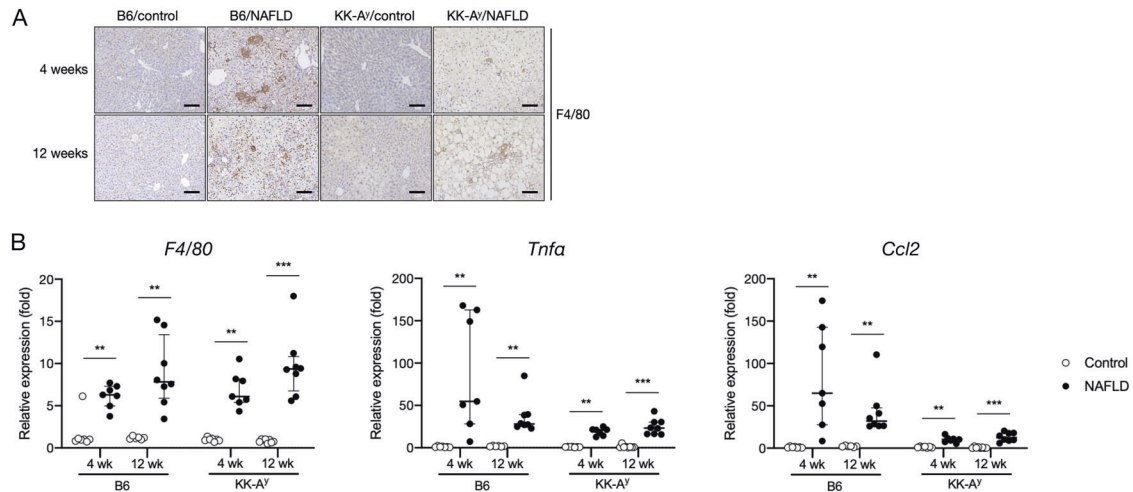


Fig. 4 Profile of liver inflammation in mice with dietary intervention. A Immunostaining for F4/80 in liver sections at 4 and 12 weeks. Scale bar, 100 μ m. B Relative expressions of *F4/80*, *Tnfa*, and *Ccl2* at 4 and 12 weeks. The expression of each gene was assessed by quantitative PCR and normalized by *Gapdh* expression. Continuous data are expressed as median with interquartile range for 6–8 mice per group. The NAFLD and control groups were compared using the Wilcoxon test. ** $p < 0.01$, *** $p < 0.001$.

NAFLD diet also showed no hepatocyte ballooning at 1 and 2 weeks, while they exhibited hepatic steatosis (data not shown). Because hepatocyte ballooning was only occasionally observed in the rodent NAFLD models, Liang et al. reported the grading system for rodent models, which omit hepatocyte ballooning but include hepatocyte hypertrophy¹⁸. Histological scoring of steatosis and inflammation was performed according to this system (Fig. 3D). The mice in the KK-A^y/NAFLD group developed remarkable steatosis at 4 weeks. Macrovesicular steatosis was mainly observed in zone 1 at

4 weeks and became more evident at 12 weeks. The mice in the KK-A^y/NAFLD group developed significant hypertrophy at 4 and 12 weeks, while they showed slight microvesicular steatosis. The mice in the B6/NAFLD group also developed significant steatosis. Macrovesicular steatosis were evident at 12 weeks. Microvesicular steatosis was evident at 4 weeks and the histological score was higher than that of the KK-A^y/NAFLD group at 12 weeks. The degree of hypertrophy was mild and the histological score was lower than that of the KK-A^y/NAFLD group at 4 weeks.

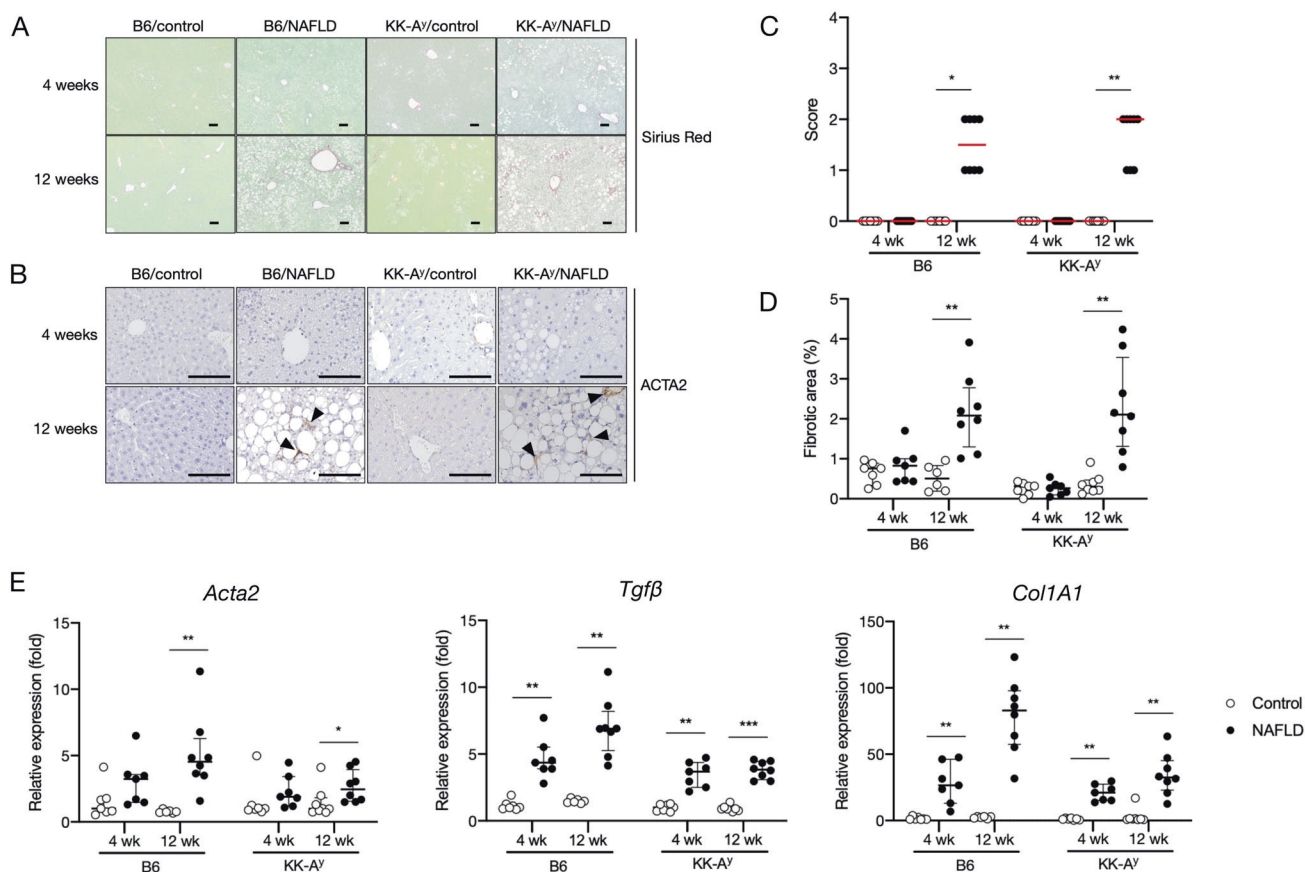


Fig. 5 Profile of liver fibrosis in mice with dietary intervention. **A** Representative images of liver sections stained with Sirius Red at 4 and 12 weeks. Scale bar, 100 μ m. **B** Histological grading of fibrosis. Each score was plotted with median (red bar) for 6–8 mice per group. All groups were compared using the Steel-Dwass test. $p < 0.05$, $**p < 0.01$, $***p < 0.001$ **(C)** Quantification of the Sirius Red-positive area at 4 and 12 weeks. **D** Immunostaining for ACTA2 in liver sections at 4 and 12 weeks. Scale bar, 100 μ m. **E** Relative expressions of *Acta2*, *Tgf β* , and *Col1a1* at 4 and 12 weeks. The expression of each gene was assessed by quantitative PCR and normalized by *Gapdh* expression. Continuous data are expressed as median with interquartile range for 6–8 mice per group. The NAFLD and control groups were compared using the Wilcoxon test. $*p < 0.05$, $**p < 0.01$, $***p < 0.001$.

Both of murine strains fed a NAFLD diet developed lobular inflammation at 4 and 12 weeks (Fig. 3A, C). Inflammation was evident in the B6/NAFLD group, showing score 3.0 at 4 weeks and score 1.5 at 12 weeks. The mice in the KK-A^y/NAFLD group showed score 1.0, while there was no significant difference between two strains (Fig. 3D). F4/80-positive cells were observed at 4 and 12 weeks in both murine strains fed a NAFLD diet (Fig. 4A). Quantitative assessment of gene expression of the liver demonstrated upregulation of inflammatory gene (*F4/80* [also known as Adhesion G protein-coupled receptor E1; *Adgre1*], tumor necrosis factor alpha [*Tnfa*] and chemokine [C-C motif] ligand 2 [*Ccl2*] at 4 and 12 weeks in both murine strains fed a NAFLD diet (Fig. 4B).

Dietary intervention rapidly causes liver fibrosis in mice

Sirius Red staining of liver section showed pericellular fibrosis at 12 weeks in both mouse strains fed a NAFLD diet (Fig. 5A). The fibrosis stage was 1.5 for the B6/NAFLD group and 2.0 for the KK-A^y/NAFLD group. These scores were not significantly different between two strains (Fig. 5B). Median fibrotic area was about 2% of total area in both mouse strains, according to quantitative morphometry assessment (Fig. 5C). No mice developed hepatic fibrosis at 4 weeks. Actin alpha 2, smooth muscle, aorta (ACTA2 [also known as α SMA])-positive cells, indicating activated hepatic stellate cells (HSCs), were observed at 12 weeks (Fig. 5D). Quantitative PCR showed upregulation of fibrotic genes (*Acta2*, *Tgf β* and *Collagen1a1* [*Col1a1*]) (Fig. 5E). Only one of the six KK-A^y/NAFLD mice had liver tumor at 37–38 weeks (data not shown).

Dietary intervention alters lipid metabolism in the liver

Quantitative assessment of hepatic gene expression demonstrated upregulation of genes related to de novo lipogenesis (DNL) (Sterol regulatory element-binding protein 1c [*Srebp-1c*], Acetyl-coenzyme a carboxylase alpha [*Acaca*], fatty acid synthase [*Fasn*] and Stearoyl-CoA desaturase 1 [*Scd1*]) at 4 and 12 weeks in the KK-A^y/NAFLD group and at 12 weeks in the B6/NAFLD group (Fig. 6A). The expression of Microsomal triglyceride transfer protein (*Mttp*), which is essential for secretion of very low-density lipoprotein (VLDL) from liver, were downregulated at 12 weeks in both mouse strains fed a NAFLD diet (Fig. 6B). Apolipoprotein B (*ApoB*), the major structural component of VLDL, were downregulated at 12 weeks in the KK-A^y/NAFLD group (Fig. 6B). The expression of Carnitine palmitoyltransferase 1A (*Cpt1a*), which is related mitochondrial β -oxidation, were affected in the B6/NAFLD group but not the KK-A^y/NAFLD group (Fig. 6C). Acyl-CoA oxidase 1 (*Acox1*), which promoted peroxisomal β -oxidation, were downregulated at 12 weeks in both mouse strains fed a NAFLD diet (Fig. 6C).

DISCUSSION

In this study, we describe a murine model for NAFLD by using diabetic KK-A^y mice and a high-fat, high-fructose, and high-cholesterol diet supplemented with cholic acid. The mice exhibit remarkable obesity, insulin resistance, and dyslipidemia, which are typical features of obese NAFLD patients. They develop severe

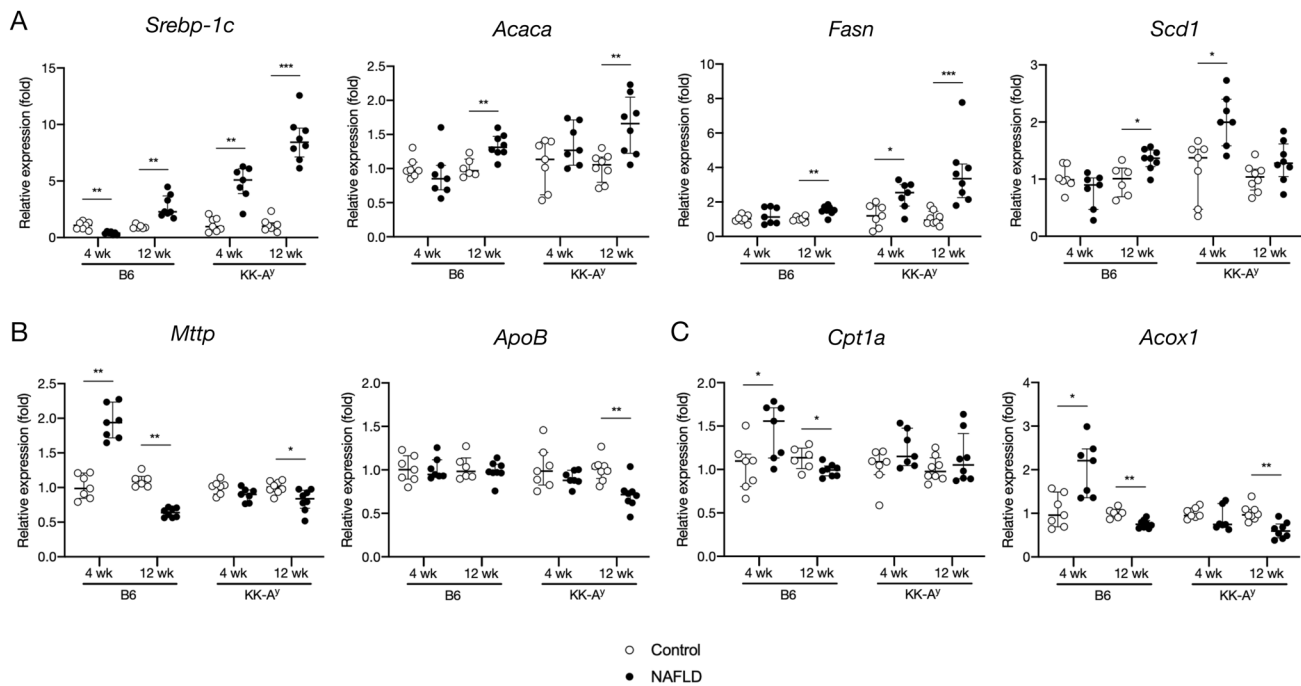


Fig. 6 Quantification of gene expression related to lipid metabolism in the liver. Relative expressions of (A) *Srebp-1c*, *Acaca*, *Fasn*, *Scd1*, (B) *Mttp*, *ApoB*, (C) *Cpt1a*, and *Acox1* at 4 and 12 weeks. The expression of each gene was assessed by quantitative PCR and normalized by *Gapdh* expression. Continuous data are expressed as median with interquartile range for 6–8 mice per group. The NAFLD and control groups were compared using the Wilcoxon test. * $p < 0.05$, ** $p < 0.01$, *** $p < 0.001$.

steatohepatitis within 4 weeks and liver fibrosis within 12 weeks. The rapid progression of disease makes the model promising as a preclinical model for human NAFLD. Interestingly, C57BL/6 J mice fed the same diet showed neither obesity nor insulin resistance. They still develop dyslipidemia, steatohepatitis, and liver fibrosis as with lean NAFLD patients.

A previous study showed that KK-Ay mice were susceptible to dietary steatohepatitis and fibrosis induced by a methionine/choline-deficient (MCD) diet, suggesting that this strain had a potential for NAFLD models. However, KK-Ay mice fed a MCD diet lost body weight similarly to other strains²⁰. The NAFLD diet used in this study accelerates weight gain and maintains the insulin resistance of the KK-Ay mice. Insulin resistance is not only a comorbidity but also an exacerbation factor of NAFLD^{8–10}. Drugs for T2DM are an emerging option for NAFLD treatment^{21–25}. Our model could be suitable for the preclinical evaluation of such drugs.

Adiponectin is a hormone secreted from adipocytes and shows the beneficial effects on lipid metabolism, insulin resistance and inflammation. Decrease of adiponectin levels are associated with the risk of metabolic syndrome. In NAFLD patients, adiponectin levels are decreased compared to control^{26–28} and low adiponectin was associated with advanced fibrosis²⁹, suggesting the relevance of hypo adiponectinemia to disease progression. Hypoadiponectinemia are observed in KK-Ay mice³⁰ and suggested to be a significant cause of dyslipidemia, insulin resistance and inflammation. This characteristic supports the potential of our KK-Ay/NAFLD model.

Recruitment and activation of macrophages has an important role in the disease activities of NAFLD³¹. The upregulation of *Ccl2*, a chemokine with a chemotactic activity for monocytes and *F4/80*, a widely used marker of murine macrophage populations, is observed in this murine model. Liver fibrosis is a common feature of chronic liver disease including NAFLD. Activated HSCs are a major source of extracellular matrices, which form the fibrotic component in the liver³². The upregulation of *Acta2*, an activation marker of HSCs (also known as α Sma), and other fibrotic genes, indicates the TGF β -driven activation of HSCs in this murine model.

The excessive accumulation of fatty acids affects the disease progression of NAFLD. In NAFLD, even though numerous fatty acids from diet or adipose tissue are delivered to liver, their synthesis from glucose and fructose by DNL is still promoted³³. Insulin accelerates DNL by enhancing the transcriptional upregulation of SREBP-1c^{34,35}, the major transcriptional regulator of the enzymes involved in DNL, including ACACA, FASN and SCD1^{36,37}. Oxysterol metabolites of cholesterol also activate SREBP-1c by affecting liver X receptor (LXR)³⁸. Our models, especially, the KK-Ay/NAFLD group, show the upregulation of *Srebp-1c* and the enzymes involved in DNL, suggesting enhanced DNL. Insulin resistance in KK-Ay mice might cause significant promotion of DNL and remarkable fat accumulation. Export of triglycerides into the blood from the liver as VLDL also regulate the amounts of fatty acids in the liver. Genetic defects of APOB, MTP that impair hepatic VLDL export cause hepatic steatosis and fibrosis in the patients with congenital hypocholesterolemia³⁹. Reduced expression of *Mttp* and *ApoB* in our models could exacerbate hepatic steatosis. Fatty acids in the liver are catabolized by β -oxidation. Impaired mitochondrial β -oxidation caused by chronic fatty acid overload leads to lipid accumulation into the liver and enhanced reactive oxygen species (ROS) in NAFLD^{40,41}. Peroxisomal β -oxidation also affects lipid metabolism in the liver. However, a role of peroxisomal β -oxidation in NAFLD pathogenesis is still unrevealed. ACOX1 is a rate-limiting enzyme in the peroxisomal β -oxidation pathway. *Acox1*-deficient and *Acox1*-mutant mice develop steatohepatitis and HCC^{42,43}, while liver-specific *Acox1* knockout protects against fatty liver caused by starvation or high-fat diet via induction of lipophagy⁴⁴. The significance of *Acox1* suppression in our models should be assessed in the future study.

Cholic acid reinforces the lipotoxicity of cholesterol by accelerating intestinal cholesterol absorption and exacerbating hepatic inflammation and fibrosis^{45,46}. On the other hand, cholic acid induce energy expenditure and improve insulin resistance^{47,48}. These preferable effects on metabolic status resulted in leanness and improved insulin resistance of B6/NAFLD mice, whereas C57BL/6 mice fed NAFLD diet without cholic acid

showed significant body weight gain in several recent studies^{49,50}. Furthermore, cholic acid also prevents hepatic triglyceride accumulation and elevated serum triglycerides by activating the farnesoid X receptor (FXR) signaling pathway. A previous report indicated that the addition of cholic acid to a high-fat diet improved steatosis and lowered serum triglycerides in KK-A^Y mice⁵¹. The abundance of cholesterol and fructose in our diet are presumed to account for the difference. The impact of cholic acid and FXR agonism should be examined based on various underlying factors. These results indicate the importance of preclinical models that possess the multiple characteristics of NAFLD.

There are also several limitations in our NAFLD model. First, hepatocyte ballooning was not observed. Hepatocyte ballooning is an important histological finding and a component of the NAFLD scoring system, such as the Brunt criteria and the NAFLD Activity Score (NAS)^{19,52}. Although some studies have reported murine models that develop hepatocyte ballooning^{12,53}, many of widely used murine models, including C57BL6 mice, that fed a MCD diet or fed a high-fat diet did not exhibit hepatocyte ballooning¹⁸. The influence of hepatocyte ballooning on disease development and progression should be elucidated in the future studies. Second, the incidence of liver tumor is low in our NAFLD model (data not shown). To clarify the mechanism of hepatocarcinogenesis by using murine models developing HCC is an important approach to conquer NAFLD-related HCC. On the other hand, advanced fibrosis is a major risk factor of HCC⁴, and the prevention of fibrosis could be another way of reducing the incidence of HCC. Our model could make a substantial contribution to studies aimed at overcoming NAFLD and its associated complication.

In summary, we established a diet-induced murine NAFLD model with a rapid development of steatohepatitis and fibrosis, bearing obesity and insulin resistance. This model could be useful for preclinical models for drug development of NAFLD.

DATA AVAILABILITY

The datasets used and/or analyzed during the current study are available from the corresponding author on reasonable request.

REFERENCES

- Eguchi, Y. et al. Prevalence and associated metabolic factors of nonalcoholic fatty liver disease in the general population from 2009 to 2010 in Japan: a multicenter large retrospective study. *J. Gastroenterol.* 47, 586–595 (2012).
- Fan, J.G. Epidemiology of alcoholic and nonalcoholic fatty liver disease in China. *J. Gastroenterol. Hepatol.* 28 Suppl 1, 11–17 (2013).
- Vernon, G., Baranova, A., Younossi, Z.M. Systematic review: the epidemiology and natural history of non-alcoholic fatty liver disease and non-alcoholic steatohepatitis in adults. *Aliment Pharmacol. Ther.* 34, 274–285 (2011).
- Younossi, Z.M. et al. Global epidemiology of nonalcoholic fatty liver disease—Meta-analytic assessment of prevalence, incidence, and outcomes. *Hepatology* 64, 73–84 (2016).
- Cholankeril, G. et al. Liver Transplantation for Nonalcoholic Steatohepatitis in the US: Temporal Trends and Outcomes. *Dig. Dis. Sci.* 62, 2915–2922 (2017).
- Younossi, Z. et al. Nonalcoholic Steatohepatitis Is the Fastest Growing Cause of Hepatocellular Carcinoma in Liver Transplant Candidates. *Clin. Gastroenterol. Hepatol.* 17, 748–755 e743 (2019).
- Estes, C. et al. Modeling NAFLD disease burden in China, France, Germany, Italy, Japan, Spain, United Kingdom, and United States for the period 2016–2030. *J. Hepatol.* 69, 896–904 (2018).
- Stepanova, M. et al. Predictors of all-cause mortality and liver-related mortality in patients with non-alcoholic fatty liver disease (NAFLD). *Dig. Dis. Sci.* 58, 3017–3023 (2013).
- Seyda Seydel, G. et al. Economic growth leads to increase of obesity and associated hepatocellular carcinoma in developing countries. *Ann. Hepatol.* 15, 662–672 (2016).
- Golabi, P. et al. Components of metabolic syndrome increase the risk of mortality in nonalcoholic fatty liver disease (NAFLD). *Medicine (Baltimore)* 97, e0214 (2018).
- Hagstrom, H. et al. Fibrosis stage but not NASH predicts mortality and time to development of severe liver disease in biopsy-proven NAFLD. *J. Hepatol.* 67, 1265–1273 (2017).
- Tsuchida T et al. A simple diet- and chemical-induced murine NASH model with rapid progression of steatohepatitis, fibrosis and liver cancer. *J. Hepatol.* 69, 385–395 (2018).
- Halaas, J. L., Boozer, C., Blair-West, J., Fidahusein, N., Denton, D. A. & Friedman, J. M. Physiological response to long-term peripheral and central leptin infusion in lean and obese mice. *Proc Natl Acad Sci USA* 94, 8878–8883 (1997).
- Lu, D. et al. Agouti protein is an antagonist of the melanocyte-stimulating-hormone receptor. *Nature* 371, 799–802 (1994).
- Iwatsuka, H., Shino, A., Suzuoki, Z. General survey of diabetic features of yellow KK mice. *Endocrinol. Jpn* 17, 23–35 (1970).
- Lee, S. et al. Comparison between surrogate indexes of insulin sensitivity and resistance and hyperinsulinemic euglycemic clamp estimates in mice. *Am. J. Physiol. Endocrinol. Metab.* 294, E261–270 (2008).
- Folch, J., Lees, M., Sloane Stanley, G.H. A simple method for the isolation and purification of total lipides from animal tissues. *J. Biol. Chem.* 226, 497–509 (1957).
- Liang, W. et al. Establishment of a general NAFLD scoring system for rodent models and comparison to human liver pathology. *PLoS ONE* 9, e115922 (2014).
- Kleiner, D.E. et al. Design and validation of a histological scoring system for nonalcoholic fatty liver disease. *Hepatology* 41, 1313–1321 (2005).
- Ikejima, K., Okumura, K., Kon, K., Takei, Y., Sato, N. Role of adipocytokines in hepatic fibrogenesis. *J. Gastroenterol. Hepatol.* 22 Suppl 1, S87–92 (2007).
- Boettcher, E., Csako, G., Pucino, F., Wesley, R., Loomba, R. Meta-analysis: pioglitazone improves liver histology and fibrosis in patients with non-alcoholic steatohepatitis. *Aliment Pharmacol. Ther.* 35, 66–75 (2012).
- Sawangjit, R. et al. Comparative efficacy of interventions on nonalcoholic fatty liver disease (NAFLD): A PRISMA-compliant systematic review and network meta-analysis. *Medicine (Baltimore)* 95, e4529 (2016).
- Musso, G., Cassader, M., Paschetta, E., Gambino, R. Thiazolidinediones and Advanced Liver Fibrosis in Nonalcoholic Steatohepatitis: a Meta-analysis. *JAMA Intern. Med.* 177, 633–640 (2017).
- Armstrong, M.J. et al. Liraglutide safety and efficacy in patients with non-alcoholic steatohepatitis (LEAN): a multicentre, double-blind, randomised, placebo-controlled phase 2 study. *Lancet* 387, 679–690 (2016).
- Kuchay, M.S. et al. Effect of Empagliflozin on Liver Fat in Patients With Type 2 Diabetes and Nonalcoholic Fatty Liver Disease: A Randomized Controlled Trial (E-LIFT Trial). *Diabetes Care* 41, 1801–1808 (2018).
- Balmer, M.L. et al. Significance of serum adiponectin levels in patients with chronic liver disease. *Clin. Sci. (Lond)* 119, 431–436 (2010).
- Polyzos, S.A., Toulis, K.A., Goulis, D.G., Zavos, C., Kountouras, J. Serum total adiponectin in nonalcoholic fatty liver disease: a systematic review and metaanalysis. *Metabolism* 60, 313–326 (2011).
- Mavilia, M.G., Wu, G.Y. Liver and serum adiponectin levels in non-alcoholic fatty liver disease. *J. Dig. Dis.* 22, 214–221 (2021).
- Leite, N.C., Salles, G.F., Cardoso, C.R., Villela-Nogueira, C.A. Serum biomarkers in type 2 diabetic patients with non-alcoholic steatohepatitis and advanced fibrosis. *Hepatol. Res.* 43, 508–515 (2013).
- Takahashi, E. et al. Differential proteome analysis of serum proteins associated with the development of type 2 diabetes mellitus in the KK-A(y) mouse model using the iTRAQ technique. *J. Proteom.* 84, 40–51 (2013).
- Marra, F., Tacke, F. Roles for chemokines in liver disease. *Gastroenterology* 147, 577–594 e571 (2014).
- Mederacke, I. et al. Fate tracing reveals hepatic stellate cells as dominant contributors to liver fibrosis independent of its aetiology. *Nat. Commun.* 4, 2823 (2013).
- Donnelly, K.L. et al. Sources of fatty acids stored in liver and secreted via lipoproteins in patients with nonalcoholic fatty liver disease. *J. Clin. Investig.* 115, 1343–1351 (2005).
- Shimomura, I. et al. Decreased IRS-2 and increased SREBP-1c lead to mixed insulin resistance and sensitivity in livers of lipodystrophic and ob/ob mice. *Mol. Cell* 6, 77–86 (2000).
- Ferre, P., Foufelle, F. Hepatic steatosis: a role for de novo lipogenesis and the transcription factor SREBP-1c. *Diabetes Obes. Metab.* 12 Suppl 2, 83–92 (2010).
- Brown, M.S., Goldstein, J.L. The SREBP Pathway: Regulation of Cholesterol Metabolism by Proteolysis of a Membrane-Bound Transcription Factor. *Cell* 89, 331–340 (1997).
- Horton, J.D., Goldstein, J.L., Brown, M.S. SREBPs: activators of the complete program of cholesterol and fatty acid synthesis in the liver. *J. Clin. Investig.* 109, 1125–1131 (2002).
- Schultz, J.R. et al. Role of LXRs in control of lipogenesis. *Genes Dev.* 14, 2831–2838 (2000).

39. Di Filippo, M. et al. Homozygous MTP and APOB mutations may lead to hepatic steatosis and fibrosis despite metabolic differences in congenital hypocholesterolemia. *J. Hepatol.* 61, 891–902 (2014).
40. Koliaki, C. et al. Adaptation of hepatic mitochondrial function in humans with non-alcoholic fatty liver is lost in steatohepatitis. *Cell Metab.* 21, 739–746 (2015).
41. Longo, M., Meroni, M., Paolini, E., Macchi, C., Dongiovanni, P. Mitochondrial dynamics and nonalcoholic fatty liver disease (NAFLD): new perspectives for a fairy-tale ending? *Metabolism* 117, 154708 (2021).
42. Huang, J. et al. Progressive endoplasmic reticulum stress contributes to hepatocarcinogenesis in fatty acyl-CoA oxidase 1-deficient mice. *Am. J. Pathol.* 179, 703–713 (2011).
43. Moreno-Fernandez, M.E. et al. Peroxisomal beta-oxidation regulates whole body metabolism, inflammatory vigor, and pathogenesis of nonalcoholic fatty liver disease. *JCI Insight* 3, e93626 (2018).
44. He, A. et al. Acetyl-CoA Derived from Hepatic Peroxisomal beta-Oxidation Inhibits Autophagy and Promotes Steatosis via mTORC1 Activation. *Mol. Cell* 79, 30–42 e34 (2020).
45. Matsuzawa, N. et al. Lipid-induced oxidative stress causes steatohepatitis in mice fed an atherogenic diet. *Hepatology* 46, 1392–1403 (2007).
46. Briand, F. et al. A 3-week nonalcoholic steatohepatitis mouse model shows elafibranor benefits on hepatic inflammation and cell death. *Clin. Transl. Sci.* 13, 529–538 (2020).
47. Watanabe, M. et al. Bile acids induce energy expenditure by promoting intracellular thyroid hormone activation. *Nature* 439, 484–489 (2006).
48. Ippagunta, S.M., Kharitonov, A., Adams, A.C., Hillgartner, F.B. Cholic Acid Supplementation of a High-Fat Obesogenic Diet Suppresses Hepatic Triacylglycerol Accumulation in Mice via a Fibroblast Growth Factor 21-Dependent Mechanism. *J. Nutr.* 148, 510–517 (2018).
49. Trevaskis, J.L. et al. Glucagon-like peptide-1 receptor agonism improves metabolic, biochemical, and histopathological indices of nonalcoholic steatohepatitis in mice. *Am. J. Physiol. Gastrointest. Liver Physiol.* 302, G762–772 (2012).
50. Xiong, X. et al. Mapping the molecular signatures of diet-induced NASH and its regulation by the hepatokine Tsukushi. *Mol. Metab.* 20, 128–137 (2019).
51. Watanabe, M. et al. Bile acids lower triglyceride levels via a pathway involving FXR, SHP, and SREBP-1c. *J. Clin. Investig.* 113, 1408–1418 (2004).
52. Brunt, E.M., Janney, C.G., Di Bisceglie, A.M., Neuschwander-Tetri, B.A., Bacon, B.R. Nonalcoholic steatohepatitis: a proposal for grading and staging the histological lesions. *Am. J. Gastroenterol.* 94, 2467–2474 (1999).
53. Asgharpour, A. et al. A diet-induced animal model of non-alcoholic fatty liver disease and hepatocellular cancer. *J. Hepatol.* 65, 579–588 (2016).

ACKNOWLEDGEMENTS

The authors would like to thank Enago (www.enago.jp) for the English language review.

AUTHOR CONTRIBUTIONS

M.N., T.C. and N.K. conceived and designed the study. T.S., T.I., M.K., R.K., A.J., M.Y., K. Kanayama, H.H. and M.N. conducted experiments and acquired data. T.S., M.N. and T. K. evaluated liver sections. H.U., N.F., K.Koroki, K.Kobayashi, N.Kanogawa, S.K., T.K., T.S., S.O. R.N., S.N., R.M. and J.K. gave administrative and technical supports. T.S., M.N., T.C. and N.Kato analyzed and interpreted the data. T.S. and M.N. drafted the paper and made figures. All authors edited and approved the final paper.

FUNDING

M.N. is supported by JSPS KAKENHI Grant Number JP19K16532.

COMPETING INTERESTS

The authors declare no competing interests.

ETHICS APPROVAL AND CONSENT TO PARTICIPATE

This paper do NOT involve human participants, human data or human tissue.

ADDITIONAL INFORMATION

Supplementary information The online version contains supplementary material available at <https://doi.org/10.1038/s41374-022-00807-6>.

Correspondence and requests for materials should be addressed to Masato Nakamura.

Reprints and permission information is available at <http://www.nature.com/reprints>

Publisher's note Springer Nature remains neutral with regard to jurisdictional claims in published maps and institutional affiliations.